Surface Science 657 (2017) 79–89

Contents lists available at ScienceDirect

Surface Science

journal homepage: www.elsevier.com/locate/susc

Dioxygen molecule adsorption and oxygen atom diffusion on clean and defective aluminum(111) surface using first principles calculations

Mathilde Guiltat[a], Marie Brut[a], Sébastien Vizzini[b], Anne Hémeryck[a,*]

[a] LAAS-CNRS, Université de Toulouse, CNRS, Toulouse, France
[b] Aix Marseille Univ, IM2NP, Fac Sci St Jérôme, F-13397 Marseille, France

ARTICLE INFO

Keywords:
Oxidation
Aluminum
DFT
Diffusion
Kinetics
Defects

ABSTRACT

First principles calculations are conducted to investigate kinetic behavior of oxygen species at the surface of clean and defective Al(111) substrate. Oxygen island, aluminum vacancy, aluminum sub-vacancy, aluminum ad-atom and aluminum terraces defects are addressed. Adsorption of oxygen molecule is first performed on all these systems resulting in dissociated oxygen atoms in main cases. The obtained adsorbed configurations are then picked to study the behavior of atomic oxygen specie and get a detailed understanding on the effect of the local environment on the ability of the oxygen atom to diffuse on the surface. We pointed out that local environment impacts energetics of oxygen atom diffusion. Close packed oxygen island, sub-vacancy and ad-atoms favor oxygen atom stability and decrease mobility of oxygen atom on the surface, to be seen as surface area for further nucleation of oxygen island.

1. Introduction

Aluminum oxides have been subject to wide number of studies focused on growth mechanisms, thermal and diffusion barrier coating properties, insulating interfaces, surface reactivity as catalysis among others [1–3] because they are of major interest for highly applicative fields such as corrosion of aluminum-based alloys, surface preparation through thermally grown oxides, high-k oxides integration in micro-electronics [4,5]. Knowing the high potential breakthroughs and reduced domestic and technological costs that could arise from the mastering and tailoring of aluminum oxide growth, this topic is still of concern. Today, oxide growth remains a not well-understood and a not controlled phenomenon: experimental and theoretical investigations reveal that aluminum oxidation is highly complex and depends on external temperature [3], substrate surface properties [6–9], crystal orientations [10–13], exhibits several ranges of velocity in growth mode [14,15], through native oxide growth to thermally grown oxide. But the growth velocity and formed oxide layer are highly dependent on the early stages of oxidation starting from first adsorption of oxygen species on the substrate to oxygen island formation and oxide nucleation. In addition, surface reactivity of aluminum oxides for further studies on polymer or organic coating to prevent corrosion, or multi-layered directly integrated materials, are hot and highly addressed topics using handmade model system usually built by assembling two material bulks which do not mimic realistic interface [16–24]. Having a realistic model-system of aluminum oxide achieved as a thermally grown oxide from the early steps of oxidation process is thus from a critical interest also for these applications and model systems.

In a recent paper, we show that kinetics are the main issue in the formation of oxygen island on the aluminum surface, which will be the center of oxide nucleus formation through a barrierless extraction mechanism [21,22]. The aim of this paper is to get insights on the kinetics of the primary steps formation of oxygen islands [22] and where and how oxygen island will begin to form, by exposing a bare Al(111) surface to oxygen molecule with a particular focus given on the subsequent behavior of adsorbed oxygen species as a function of its local structure when considering increasing coverage and influence of presence of defects using a first-principles calculations approach.

Previous theoretical and experimental approaches of primary stages of oxygen molecule adsorption on Al surfaces reveal a systematic dissociation on the clean Al(111) surface, [6,24–37]. This dissociation is due to a charge transfer inside the dioxygen molecule leading to the partial occupancy of the anti-bonding orbitals: the molecule goes through different electronic states known as $O \rightarrow O_2^- \rightarrow O_2^{2-}$ [29,31,32,38]. In the literature, the dissociation occurs on the surface that could lead to abstraction mechanism giving rise to monomer on the surface [32], or could result in the separation of oxygen atoms in close neighborhood between one and three Al interatomic spacing [35] or by more than 80 Å [21,39], thus appearing still as an unclear issue. Actually, isolated oxygen atom are observed on aluminum surface and

* Correspondence to: Laboratoire d'Analyse et d'Architecture des Systèmes, LAAS-CNRS, Toulouse, France.
E-mail address: anne.hemeryck@laas.fr (A. Hémeryck).

http://dx.doi.org/10.1016/j.susc.2016.11.010
Received 12 August 2016; Received in revised form 25 November 2016; Accepted 26 November 2016
Available online 30 November 2016

explained by the high-energy release incoming from the adsorption of molecular oxygen. This high-energy release appears to give an enhanced velocity to adsorbed oxygen atom on the surface that will consequently exhibit a high mobility on the surface and long scale displacement. This high mobility observed right after the dissociation will result in a 'hot atom' behavior as referred in many experimental publications [27,35,39,40]. However, this cannot be observed in first-principles calculations because non-adiabatic effects are not taken into account, whereas they cannot be neglected [32]. But oxygen atoms diffuse on the surface forming close-packed oxygen islands thanks to thermal activated moves and favorable energy interaction. This point is relevant and stimulates few discussions about activation barriers that drive oxygen island formation [21,23,24,33,41–44], because of the difficulty to estimate the activation barrier experimentally. Large scale modeling approaches based on Monte Carlo methodologies have been developed to simulate primary steps of oxidation in order to take into account kinetics [33,41,42,45]. Furthermore, structural defects can also have a drastic effect on the activation barriers that could affect kinetics of the oxygen islands formation and also their number and size on the surface. Defects are observed experimentally on the surface [21,40,46], but have not been subject of studies to our knowledge, whereas it is clear that when environment changes locally, it will impact the chemical dissociation and adsorption mode of the oxygen molecule [22,36,37,41,45,47–49].

With such non-elucidated points about kinetics and surface defects influence, we combine a study on molecular oxygen adsorption with atomic oxygen behavior investigation, on clean and defective Al(111) surfaces for a complete overview. The main focus will be the investigation of the ability of oxygen atom to move on the surface as a function of its local environment and see how activation barriers of oxygen atom diffusion are affected. Among considered defects, we investigate aluminum vacancy, aluminum sub-vacancies, aluminum ad-atoms, and aluminum steps defects. This paper based on Density Functional Theory based calculations (DFT) is organized as follows: Adsorption of oxygen molecule on Al(111) is first addressed, then thermodynamics and kinetics of atomic oxygen are discussed with an increasing oxygen coverage by considering isolated oxygen atom and an existing oxygen atoms island [43,50,51]. This has to be considered because oxygen island has to be first formed on the surface to allow oxide to grow [6,21,22,29,33,52]. In the second part of the paper, the adsorption of oxygen molecule is performed as detailed in the first part for Al(111) containing defects: vacancy, sub-vacancy, ad-atom, terrace. Kinetics of isolated oxygen atom moving on these defective surfaces is then discussed.

2. Computational details

Calculations are based on Density Functional Theory (DFT) [53] with the Perdew-Burke-Ernzerhof functional in the Generalized Gradient Approximation (PBE-GGA) [54] as implemented in VASP 5.3 (Vienna Ab initio Simulation Package) [8,55–57]. We used a plane wave basis set for the Kohn-Sham Bloch functions, with a cut off energy of 400 eV to account for valence electrons. Ions are relaxed with a conjugate-gradient algorithm. The sampling of the Brillouin zone was performed using a Monkhorst-Pack [9] mesh of 2×2×1 k-points. The nudged elastic band (NEB) method [10,11,58] was used to determine activation barriers along reaction paths of atomic oxygen species. The aluminum(111) slab is built as an orthorhombic supercell of (4×2) surface unit cells. A vacuum zone of 15 Å is added following the z-axis, in order to model the surface. The system contains 96 atoms distributed in 6 layers of 16 atoms corresponding to slab dimensions of 11.43×9.90×25.00 $Å^3$. Al atoms at the bottom of the cell are kept fixed during geometry optimizations, reproducing thereby the bulk behavior. All other atoms are free to relax.

This slab is used throughout the paper in order to study both atomic and molecular oxygen species adsorption. Adsorption is performed by considering atomic oxygen in a singlet state whereas molecular oxygen is initially set in a triplet state, with a spin state free to relax. In all adsorption mechanism, oxygen species are placed at 2 Å above the Al(111) surface and then are fully relaxed. Considering the simulated coverage and surface dimensions, the used slab has been validated as large enough to avoid any interaction between periodic slabs during both adsorption and diffusion investigations.

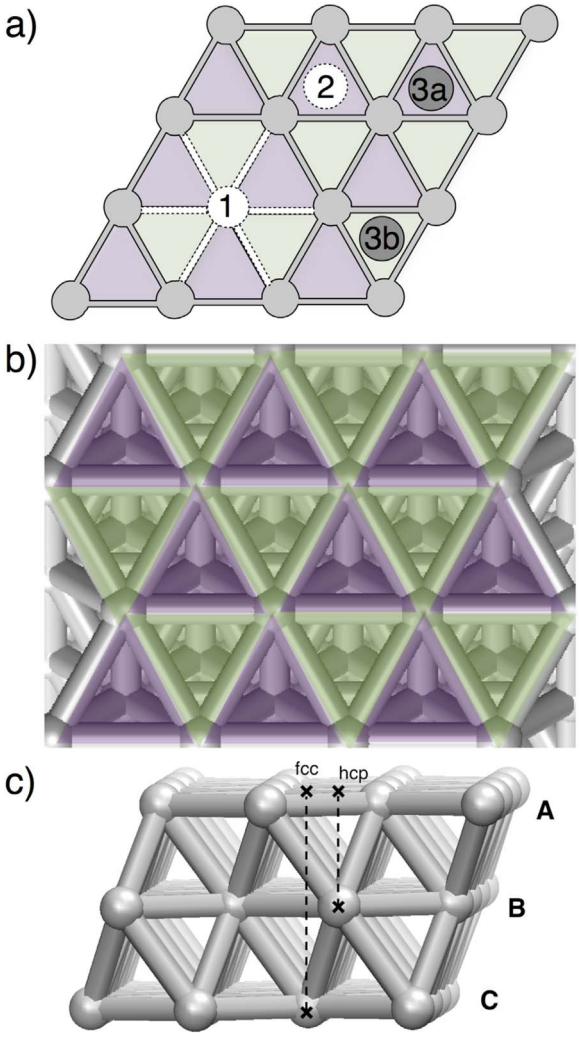

Fig. 1. (a) Schematic top view of Al(111) used throughout the paper where hcp, fcc, vacancy, sub-vacancy and ad-atom are represented. This color scheme will be used throughout the paper into the schematics. Grey circles represent aluminum atom. White circles are for vacancies and dark grey one are for ad-atoms. (b) is provided to highlight fcc sites represented by green triangles and the hcp ones in purple, on top view. (c) is a side view of the three topmost layers of our simulation slab to explain fcc and hcp use as epitaxial and anti-epitaxial growth sites. (For interpretation of the references to color in this figure legend, the reader is referred to the web version of this article.)

Using this (111) oriented aluminum surface-model (Fig. 1), the deposition of dioxygen molecule and oxygen atom on both clean surface and defective surfaces are performed. For each surface, the defect formation energies have been calculated as $\Delta H_f = E_{defective\_bulk} \pm E_{Al} - E_{clean\_bulk}$ where $E_{defective\_bulk}$ is the total energy of the defective bulk (see Fig. 1), E_{Al} is taken as the reference energy of the atomic aluminum calculated from the bulk and E_{clean_bulk} is the energy of perfect Aluminum slab (111). The studied Al(111) surfaces are:

- A perfect Al(111) surface considered as the reference system.
- Defective surfaces containing Al Vacancy and Al sub-vacancy defects schematized as #1 and #2 on Fig. 1a. Formation energies of such defects are respectively 0.80 eV and 0.87 eV [46]. Other defective

surfaces contain Al ad-atom defect, the formation energies are 0.85 eV when generated from a kink site at the edge of a terrace defect as will be discussed in the following and 1.79 eV if formed as a Schottky defect.

In the following, the reaction energies ΔH are calculated as follows :

$$\Delta H = E_{total} - E_O - E_{bulk}$$

With:

- E_{total} the total energy of the system in a given adsorbed configuration.
- E_O the reference energy of an atomic oxygen calculated from ½ of the molecular oxygen or of an molecular oxygen depending on the considered adsorbed specie.
- E_{bulk} the reference energy of smooth or defective Aluminum slab.

3. Oxygen behavior on clean aluminum surface

3.1. Dioxygen molecule adsorption

Primary calculations are focused on the adsorption of molecular oxygen species on perfect aluminum surface [21,24,29,30,40,43,50,59,60]. Several starting orientations and positions for the dioxygen molecule have been tested and all the final positions are provided on Fig. 2. Initial configurations of the dioxygen molecule have been chosen with the respect of the surface topology (above topmost atom or fcc site or hcp sites) by considering either horizontal or vertical orientations centered or shifted from the center of adsorption sites. As previously reported in literature, the adsorption mechanism of dioxygen is dissociative, barrierless and brings a great energy gain of ΔH=-9.85 eV [24,37].

Starting positions are in Fig. 2a: number given inside this starting position is provided to establish the correlation with final positions given in Fig. 2b. As can be observed, several starting different configurations can result in a same final configuration. Circles with two rings represent vertical molecules; two circles and a stick represent the horizontal ones.

The more stable position contains two adsorbed oxygen atoms on close fcc sites, as first neighbors (d=2.90 Å) and referred as #1 in Fig. 2b. This final configuration is obtained when the dioxygen molecule is placed horizontally, centered or shifted (along the x-axis), above the Al surface and associated with a reaction enthalpy large of ΔH=-9.85 eV. Other stable position exhibits one oxygen atom on a fcc site and the other on a hcp site also in close vicinity (d=3.31 Å), where oxygen atoms are second neighbors. This position is reached when the dioxygen molecule is placed vertically or parallel (along the y-axis) on the surface aluminum between the two final sites, or vertically put above a hcp site. The energy gain for this position is ΔH=-9.32 eV. The third more stable position is obtained with the dioxygen molecule placed horizontally (along the x-axis) and centered above a hcp site: here one oxygen atom is adsorbed on a fcc site and the other on a hcp site on third neighbor. The energy gain for this position is ΔH=-9.16 eV. Here, we notice that oxygen atoms are in hcp and fcc sites as observed in #2 but further from each other. This indicates a supplementary favorable interaction existing when oxygen atoms are in close neighborhood as in configuration #2 which does not exist anymore in configuration #3. This favorable interaction is attributed to a larger electrostatic interaction coming from higher charge transfers between adsorbed oxygen atoms and their surrounding aluminum atoms, stabilizing the system when the two oxygen atoms are adsorbed as first neighbors. A fourth stable position is obtained when the dioxygen molecule is placed above a fcc site, vertically or parallel (along the x-axis) resulting in two oxygen atoms adsorbed on two hcp sites as first neighbors. We notice here that hcp is a less stable position compared to fcc site when comparing this final adsorbed configuration with the most

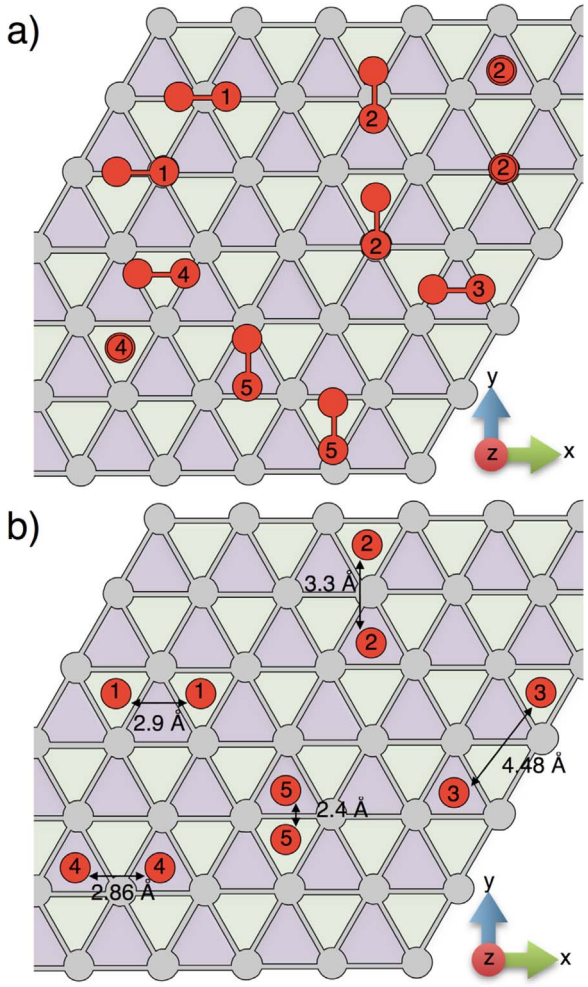

Fig. 2. Schematic top views of dioxygen molecule deposited on smooth aluminum surface. (a) Starting positions above the surface and (b) final dissociated and adsorbed configurations where identical numbers belong to the same molecule. Molecules with identical numbers on starting positions lead to the same final configuration in (b). Energy gains of configurations (b) are provided in Table 1.

stable one, i.e. two adsorbed oxygen atoms on fcc sites. This adsorbed position corresponds to ΔH=-9.06 eV. The last position and also the less stable observed in this study is obtained when one oxygen atom is on hcp site and the other on fcc site at a distance of d=2.40 Å, which is a smaller distance compared to the most favorable adsorbed configuration. Here, the two oxygen atoms are too close and a repulsive energy destabilizes the system. This last position is obtained with the dioxygen molecule placed horizontally (along the y-axis), centered above a hcp and a fcc site. The energy gain is ΔH=-8.96 eV.

In conclusion, fcc sites are the most stable on the Al(111) surface and first neighbor interactions are favorable.

But considering high energy released during the adsorption, it is shown that oxygen atoms once dissociated and adsorbed on the surface will migrate rapidly due to this extra energy that will enhance their mobility on the surface as 'hot atom' behavior [29,31,35,37,39,60]. At this stage, one can consider that atomic specie exists on the surface also as an isolated adsorbed state as observed experimentally [40] and a detailed study on oxygen species as an isolated atom has to be considered.

3.2. Atomic oxygen adsorption

Considering previous conclusions, the dissociation of dioxygen molecule on Al(111) is observed at the primary steps of adsorption.

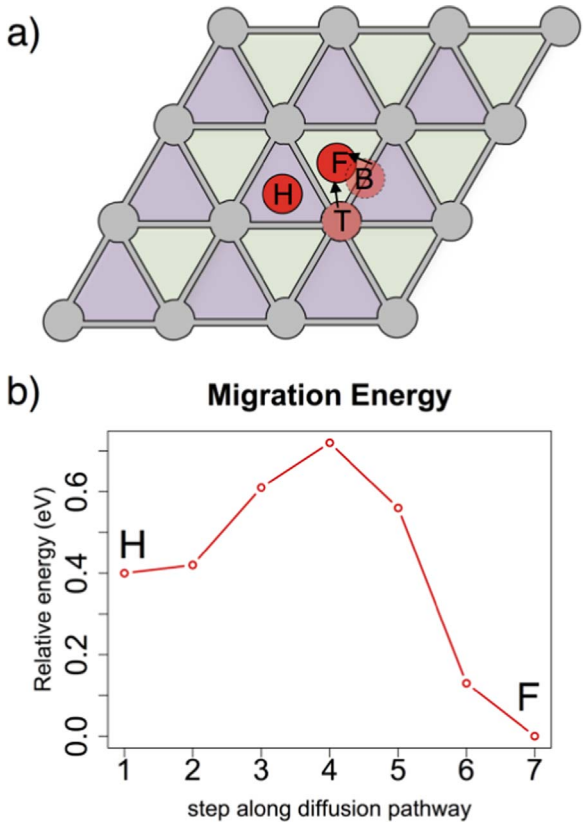

Fig. 3. (a) Schematic top view of oxygen atoms deposited on clean Al(111) surface. Oxygen atoms are schematized by red circles and aluminum atoms are grey. (b) Activation barrier associated to the migration of one oxygen atom on the clean Al(111) surface between the hcp and fcc sites. (For interpretation of the references to color in this figure legend, the reader is referred to the web version of this article.)

In this context, a careful study has been conducted on the behavior of a single oxygen atom on the Al(111) surface: - as an isolated atom moving on the surface and - as a function of larger coverage since favorable interaction between oxygen atoms when adsorbed in close neighborhood has been discussed above. The study is carried out with the goal to get insights on kinetics of oxygen diffusion and discussing clustering effects on the surface.

The stability of the isolated atomic oxygen on all possible existing configurations hcp, fcc, top and bridge sites is first studied. Fig. 3a illustrates the adsorption of a single oxygen atom above the four characteristic sites of the (111) fcc-like surface, respectively top, bridge, fcc and hcp, referred as T, B, F and H [22–24,35]. Only two sites are stabilized where fcc site (ΔH=-4.82 eV) appears as energetically favored by -0.40 eV compared to the hcp site (ΔH=-4.41 eV) in a good agreement with the dissociated adsorbed states in fcc and hcp configurations (#1 vs #4 in Fig. 2b). The atomic study confirms that top and bridge configurations as adsorbed states do not exist on Al(111) surface and finally result in fcc adsorbed state. Nevertheless, we performed constraint relaxations by keeping frozen x and y coordinates of the oxygen atom in both bridge and top positions on order to estimate the potential energy surface. These calculations reveal that top position is less favorable by 0.16 eV compared to the bridge configuration. The bridge configuration will thus be used as the saddle point to characterize the most probable minimum energy path of oxygen atom diffusion between fcc and hcp sites. Activation barriers are calculated below.

To go further and get clues on the kinetics associated to the diffusive behavior of an isolated oxygen atom, we characterize the diffusion between the two observed stable adsorption sites fcc and hcp in close neighborhood. The minimum energy path is illustrated on the Fig. 3b and the associated activation energy is given on Fig. 3c.

From the fcc site, oxygen atom must overcome an activation barrier large of 0.72 eV to move from fcc site toward hcp one (Fig. 3c). The backward migration reaction from hcp to fcc site is characterized by an activation barrier of 0.30 eV. Both the disparity when regarding sites stability and the lower activation barrier from hcp to reach a more stable fcc site lead us to conclude that fcc site is favored [12,21,40,61].

3.3. Increasing coverage: migration toward formation of oxygen islands

The same study focused on the atomic oxygen migration is performed with an increasing coverage of oxygen atoms by considering already formed oxygen island on the surface in order to investigate in details the favorable interaction effect on the ability of oxygen atom to diffuse on the surface. This favorable interaction has been revealed in the molecular adsorption study.

First, a static investigation is first performed: the energies of two oxygen atoms deposited on fcc sites on close first neighborhood (d=2.90 Å) or distant by 5.73 Å from each other are compared: We respectively obtained -9.85 eV and -9.66 eV for adsorption energies. The -0.19 eV difference between these adsorption energies can thus be explained by the favorable interaction existing between oxygen atoms stabilizing the system with a contribution of -0.10 eV per atom. As an interacting energy term exists, we evaluate its effect on the ability of oxygen atom to diffuse from a close-packed three oxygen atoms island moving to an isolated state between different configurations (see Fig. 4a):

A. The triangle, as a close-packed compact configuration, where oxygen atoms are located on sites #1, #2 & #3 on Fig. 4a. In this configuration, the adsorption energy is -15.06 eV. The contributing interaction energy to the value is estimated to be -0.60 eV, with six interaction terms to be considered similarly to the contribution of -0.10 eV per atom as previously calculated.
B. The L-shape, where atoms located on sites #1, #2 and on sites #2, #5 are first neighbors but atoms located on sites #1, #5 are distant by 4.99 Å. In this configuration, the adsorption energy is large of -14.83 eV. This lower adsorption energy is obtained due to a reduced interaction energy (estimated at -0.37 eV). This energy difference corresponds to the broken bonds compared to the triangle configuration, indicating that oxygen atom has no more interaction with the other oxygen atom located as its second neighbor.
C. The line configuration, where oxygen atoms are adsorbed on sites #1, #2 & #7 with sites #1, #2 and #2, #7 are shown as first neighbors and sites #1, #7 are distant by 5.77 Å, with an adsorption energy of -14.88 eV. The interaction energy is -0.42 eV, which is close to the previous one, where no-interaction exists between the furthest oxygen atoms of the line configuration.
D. So-called Isolated oxygen configuration (adsorbed states on sites #1, #2, #8), where one oxygen atom is isolated from the two oxygen atoms adsorbed on close sites. Sites #1, #2 are first neighbors. Here, the adsorption energy is the weakest with -14.70 eV. The interaction energy is -0.24 eV, revealing only two oxygen atoms in interaction, and a third isolated one.

These configurations confirm the favorable interacting energy between oxygen atoms when adsorbed as first neighbors. This energy can be quantified and is large of -0.2 eV per pair of interacting oxygen atoms. This observation enables us to assume that oxygen island will be favorably formed on the surface on Al(111) substrate.

Considering those configurations, we explore the migration of one oxygen atom leaving a compact triangle configuration (A) to reach an isolated state (D). This path is explored as a multi-steps reaction by moving one oxygen atom of the A configuration step-by-step through fcc and hcp sites as identified previously. This multi-steps migration

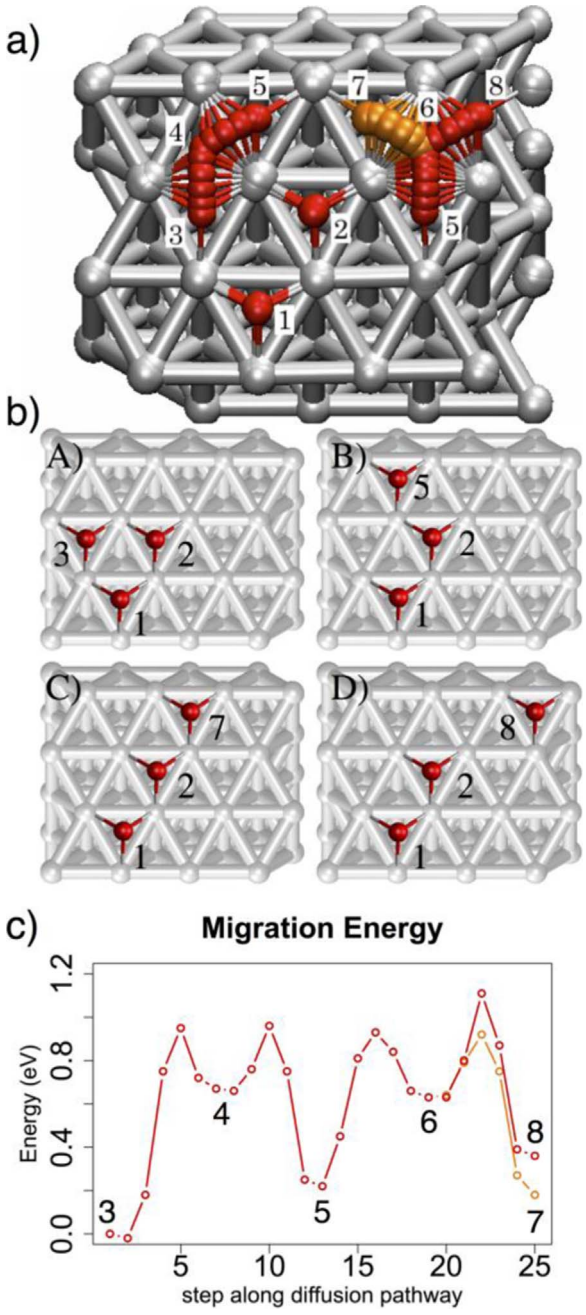

Fig. 4. (a) Top view of the migration of one oxygen atom around an island composed of two other oxygen atoms. (b) Top views of fcc configurations reached during the migration. (c) Minimum energy path corresponding to the migration of the figure (a). The red line corresponds to the red oxygen migration. The orange one corresponds to orange oxygen migration. (For interpretation of the references to color in this figure legend, the reader is referred to the web version of this article.)

path is depicted on Fig. 4: here, oxygen atoms located on sites #1 and #2 are kept fixed and the oxygen atom initially located on site #3 diffuses until position #8. So-called steps are thus associated to the possible adsorbed positions encountered by the moving oxygen atom exploring the space from A to D configurations. This moving oxygen atom will pass by L configuration when adsorbed on site #5 and line configuration when adsorbed on site #7. Oxygen atom migrates from fcc to fcc sites through hcp sites #4 and #6, as depicted in Fig. 4a. Both positions #5 shown on Fig. 4 are equivalent considering the neighborhood; they were used because of the periodic conditions of our simulation cell. Minimum energy path is shown on Fig. 4b.

The first diffusion from #3 to #4, corresponding to a displacement from fcc to hcp, highlights an activation barrier of 0.95 eV. Compared to the single oxygen atom migration in Fig. 3c, we observe an increase of the activation barrier large of 0.20 eV indicating that compact configurations are favored, thanks to a favorable oxygen-oxygen interaction. Starting from configuration (A), it will not be favorable to dissociate triangle configuration and few oxygen atoms will be able to leave compact adsorbed structure because of the high activation barrier of 0.95 eV expect under high temperature condition.

In the following, we observe that the migration of oxygen specie moving around an existing island has the same behavior as an isolated oxygen: when oxygen atom moves from site #4 to site #5 the same activation barriers (0.30 eV and 0.73 eV) are observed as the ones determined in Fig. 3c. This shows that an interaction between two oxygen atoms has short-range influence: oxygen atom on position #4 does not see anymore the oxygen atom located on position #1 as confirmed by the total energy discussed before.

From the L-shape, when moving atom is adsorbed on site #5, two different pathways are investigated: – where oxygen atom can move around the island (from #5 to #7) to form the line configuration or – where oxygen atom can leave the island (from #5 to #8) as the described isolated oxygen configuration. When oxygen atom diffuses from #5 to #7, through #6, activation barriers are the same as those observed in the case of isolated atom as in migration from #4 to #5 in Fig. 4a and b, confirming the short range interaction between oxygen atoms. Oxygen atom will thus have the same ability to diffuse as an isolated state as when moving around an oxygen island.

On the contrary and interestingly, when oxygen atom is moved away from an oxygen island, a raise in the activation barrier is observed from the hcp to fcc sites: the activation barrier from #6 to #8 increases to the value of 0.48 eV and a destabilization of the final configuration by 0.18 eV is observed.

As previously conducted [22], dragging an oxygen atom outwards from a larger oxygen atoms island (from four oxygen atoms), lead to a rise of the activation barrier to 1.22 eV, 0.27 eV higher than the migration between positions #3 and #4 in the case of three oxygen atoms island. This energy increase reaches 1.30 eV for five oxygen atoms island and more.

Considering kinetics and energetics, these calculations reveal the tendency of oxygen atom to form close-packed oxygen island on the surface of Al(111) at low coverage. Nevertheless, interestingly we observe that oxygen atom exhibits the same kinetics to move around the oxygen island without going away as the ones observed as isolated state. These conclusions are experimentally observed, with the formation of geometrical clusters at low coverage in agreement with highly symmetrical Al(111) pattern [21].

4. Oxygen specie adsorption on defective aluminum surfaces

4.1. Aluminum surface containing a vacancy

A similar detailed study is realized on a defective surface containing a vacancy on the topmost surface symbolized by a white circle on Fig. 5: on this defective surface, molecular oxygen specie is adsorbed above the vacancy and atomic oxygen behavior is investigated from adsorbed state.

In the case of molecular oxygen adsorption above the vacancy defect, at a first glance, one can observe that only one starting configuration leads to a non-dissociative adsorbed case (#7 on Fig. 5b) when initially molecular oxygen is placed above the vacancy site, in line with a Al–Al bond centered above a fcc site inside the vacancy site. The final non-dissociated state is a metastable state with ΔH=-3.90 eV as a bridge configuration where oxygen molecule is adsorbed as a peroxy bridge on two aluminum atoms around the defective site. A dissociative adsorption is observed in all other tested cases. Other remarkable configurations (#2, #4 and #5) exhibit bridge position where only one oxygen atom is bonded to two aluminum

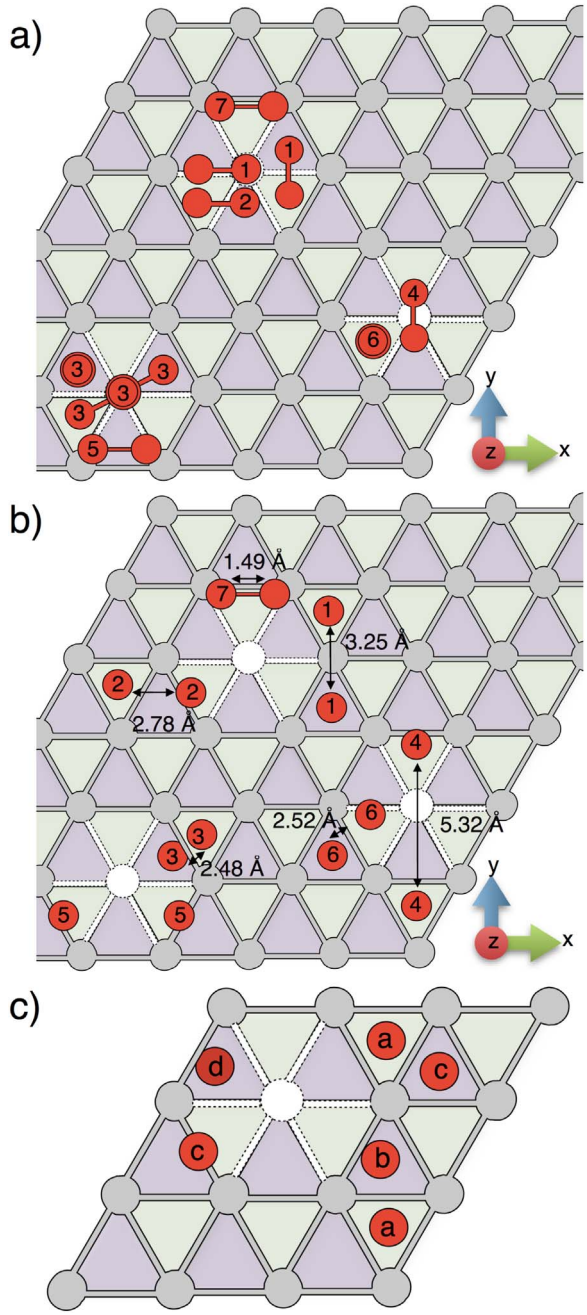

Fig. 5. (a) Schematic top views of dioxygen molecule deposition on the aluminum surface containing a vacancy schematized by a white circle and (b) final dissociated and adsorbed configurations where identical number on each dissociated oxygen atoms belongs to the same molecule. Molecules with identical number on starting positions lead to the same final configuration. Adsorption energies of those configurations are provided in Table 2. (c) Schematic top view of the deposition of atomic oxygen on the aluminum surface containing a vacancy. Identical letters are oxygen atoms with the same adsorption energy given in Table 3.

atoms around the vacancy. The bridge configuration is obtained when adsorption occurs above the vacancy defect and close to an available hcp surface site. The first conclusion is that vacancy stabilizes bridge configurations whereas the configuration was not reachable on non-defective surface. Configuration #5 is obtained with the molecule placed in the same way as the molecule #7, but above a hcp site of the vacancy, in line with Al–Al bond and with a neighboring surface fcc site. Such a position leads to the molecule dissociation above the vacancy where each oxygen atom goes on a bridge position, on the closest neighboring hcp sites of the aluminum surface.

Configurations #3 and #6 result in dissociated oxygen atoms with one oxygen atom adsorbed on a surface site surrounding the vacancy and the other one inserted underneath the topmost layer. Both configurations characterized by an insertion inside the vacancy defect exhibit different adsorption energies large of -0.80 eV that can be explained by the obtained adsorption sites: in one case the oxygen atom on the surface is on fcc and the second is located inside the vacancy as on hcp site (#3), in the other case one oxygen atom is adsorbed on hcp on the surface and the other is adsorbed inside the vacancy between a fcc and a hcp site (#6). The difference on the energetic gains observed between #3 and #6 income in one hand from the higher stability of the fcc site on the surface compared to hcp site even close to a vacancy and on the other hand mainly because of the destabilization of the configuration #6: actually the oxygen atom inside the vacancy is on a bridge-like configuration, a non stable configuration, as will be discussed below, which only exists when another oxygen atom is nearby.

Interestingly, we observe that energy gain large of -9.53 eV of the configuration #1 is more favorable compared to the adsorption on perfect surface with the configuration #2 on the Fig. 2 at -9.32 eV. This shows that vacancies stabilize oxygen atoms and so this kind of defect is more favorable than the clean surface.

To investigate the stability of the neighboring fcc or hcp adsorption sites at the neighborhood of a vacancy, we relax the atomic oxygen specie by placing it above a vacancy. In the following we also perform a static study based on final adsorption configurations observed in Fig. 5c. Results for the atomic oxygen are given in Table 3.

It is mainly observed that the oxygen atom relaxes favorably in either fcc or hcp sites on the surface layer as first neighbors of the vacancy. The stability of fcc sites is not affected by the presence of an existing vacancy even if oxygen atom is located as first and second neighborhood from this vacancy (See configuration a on Fig. 5c). The oxygen adsorption energy is nearly the same as on the clean surface with ΔH=-4.85 eV. On the other hand, hcp sites are affected, since a stabilization of the oxygen atom is obtained with an adsorption energy large of ΔH=-4.65 eV and -4.53 eV when oxygen atom is placed on a hcp site in close neighborhood of vacancy, compared to -4.41 eV for the clean surface. This energetic gain regarding the stability of the hcp site nearby a vacancy defect explains the energy gain observed in configuration #1 on Fig. 5a and b. Interestingly, we observe that the bridge configuration is stabilized when oxygen atom is adsorbed above the vacancy and close to hcp site.

The last position is obtained with the oxygen atom adsorbed inside the vacancy, above a hcp site inside the vacancy (See configuration d on Fig. 5c). It is placed in the center of a triangle formed by two aluminum atoms of the surface and the one in the bottom layer, so its position is slightly underneath the surface layer. It is the less stable with ΔH=-4.36 eV.

Furthermore interestingly, we do not succeed in getting a bridge configuration stabilized between a fcc site and the vacancy, this one reaching an adsorbed fcc configuration as in Fig. 5c. As well we do not succeed in inserting an oxygen atom on a fcc site inside the vacancy as reached when molecular adsorption occurs: an oxygen atom directly inserted on a fcc position inside the vacancy between the topmost layer and the sub-surface layer, based on the observation of the final configuration #6 on Fig. 5b leads to a surface reconstruction: the oxygen atom goes on a fcc surface site configuration and a sub-vacancy is created, where an aluminum atom of the sub-surface layer moves toward the topmost layer, healing the surface. Here, we notice that the

Table 1
Energy gain after the adsorption of the dioxygen molecule, in relation with the Fig. 2.

Positions (#)	1	2	3	4	5
ΔH (eV)	-9.85	-9.32	-9.16	-9.06	-8.96

Table 2
Energy gain after the adsorption of the dioxygen molecule above the vacancy, in relation with the Fig. 5b.

Positions (#)	1	2	3	4	5	6	7
ΔH (eV)	-9.53	-9.43	-9.31	-9.16	-8.85	-8.67	-3.90

Table 3
Energy gain after the adsorption of the oxygen atom close to a vacancy, in relation with the Fig. 5c.

Positions (#)	a	b	c	d
ΔH (eV)	-4.85	-4.65	-4.53	-4.36

Table 4
Energy gain after the adsorption of the dioxygen molecule close to a sub-vacancy, in relation with the Fig. 7b.

Positions (#)	1	2	3
ΔH (eV)	-9.70	-9.47	-9.37

Table 5
Energy gain after the adsorption of the dioxygen molecule close to a sub-vacancy, in relation with the Fig. 7c.

Positions (#)	a	b	c
ΔH (eV)	-4.87	-4.78	-4.44

spontaneous adsorption of oxygen atom as inserted into the vacancy by replacing missing aluminum atom is never observed. Even if the oxygen atom is directly placed into the site of the missing aluminum atom, we observe that the oxygen atom adsorbed in a as-like fcc site in the sub-surface layer with an energy gain of -4.13 eV, lower compared to other adsorbed configurations on the surface.

In the following part, we also study the influence of a vacancy on the atomic migration of oxygen atom in close vicinity of the vacancy. NEB calculations with oxygen atom moving around the vacancy have been performed and are shown in Fig. 6.

The studied migration starts from a hcp site in direct contact with the vacancy in #1 on Fig. 6a to reach a fcc site named #2. The encountered migration barrier is large of 0.55 eV to go far from the vacancy toward a fcc site #2. This energy barrier is larger by 0.25 eV compared to the case of clean surface (Fig. 3b), due to the stabilization of the hcp site in the vicinity of the vacancy (see Fig. 5c). Then from fcc site #2, oxygen atom will migrate around the vacancy on a hcp site nearby as #3 and #4, through a determined activation barrier of E_{ac}=0.69 eV. The migration around the vacancy will be favored energetically, with the position #4 more stable by -0.08 eV compared to #3, so that an oxygen atom located on #3 will preferentially go back toward #2 with an energetic barrier E_{ac}=0.27 eV, compared to going away from the vacancy (E_{ac}=0.34 eV). Then from #4, oxygen atom can move toward the fcc site #5 with E_{ac}=0.41 eV. When oxygen atom is located on site #5, it is surrounded by activation barriers of nearly 0.72 eV, which are the same obtained as on clean part of the surface. It confirms here the local effect of the vacancy only on the stability of hcp site and not on the fcc. Then, in position #6 oxygen atom still feels the vacancy since its stability is more stable by -0.10 eV compared to the one on clean surface. Here, the diffusion will be easier to leave the vacancy area (E_{ac}=0.22 eV) than to maintain a diffusion process around the vacancy to the position #5 (E_{ac}=0.40 eV).

We observe that vacancy will stabilize hcp sites directly located in the close area of the vacancy and will notably slow down the diffusion of the oxygen atom when it is adsorbed on the neighboring sites. A

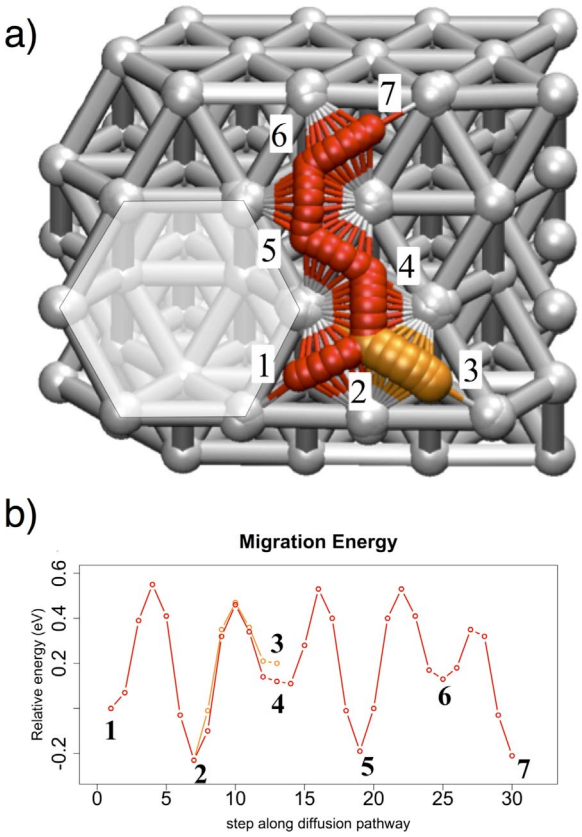

Fig. 6. (a) Top view of migration pathway of the oxygen atom on the aluminum surface next to the vacancy (b) energies associated to the oxygen migration pathway.

stabilization of the hcp site large of -0.25 eV as first neighbor and -0.15 eV as a second neighbor associated to an increase of the activation barrier large of 0.25 eV were observed. Once the oxygen atom leaves the close neighborhood of the vacancy, its diffusion ability tendency is the same as the clean surface.

4.2. Aluminum surface with vacancy in sub-surface layer

The sub-surface vacancy defect is formed by removing one oxygen atom of the sub-surface layer, i.e. under a hcp site of the surface. In the following pictures, the sub-vacancy is symbolized with a white dashed line circle in Fig. 7.

For all the tested starting positions, the dioxygen molecule dissociates on the surface. The fcc sites of configuration #1 are lightly destabilized with ΔH=-9.70 eV, instead of -9.85 eV on the clean surface. For both configurations #2 and #3, we observe an energy gain large of -0.41 eV compared to adsorption on clean surface (see Fig. 7). Here, we note that a change in energy is associated to the presence of a vacancy in sub-surface layer that stabilizes hcp site right above the sub-vacancy. This energy gain is accompanied by a diminution of 0.02 Å to 0.10 Å of the O–Al bond. Finally, the configuration #3 remains the less stable because of the proximity of the two oxygen atoms. This is highlighted with bond deformation where bonds between the oxygen atoms are longer by ~0.02 Å while the other ones are shortened by 0.05 Å to 0.10 Å. (Tables 6 and 7).

To get a better understanding of sub-surface vacancy and discriminate the role of each kind of surface site, an atomic oxygen specie has been placed directly above several fcc and hcp sites distinct from each other by their distance from the vacancy from first neighbor to third neighbor. These sites are classified by ΔH on the Fig. 7c. The most stable site is the fcc in second neighbor (configuration a on Fig. 7c) with ΔH=-4.87 eV where oxygen atom adsorbed on this site does not feel

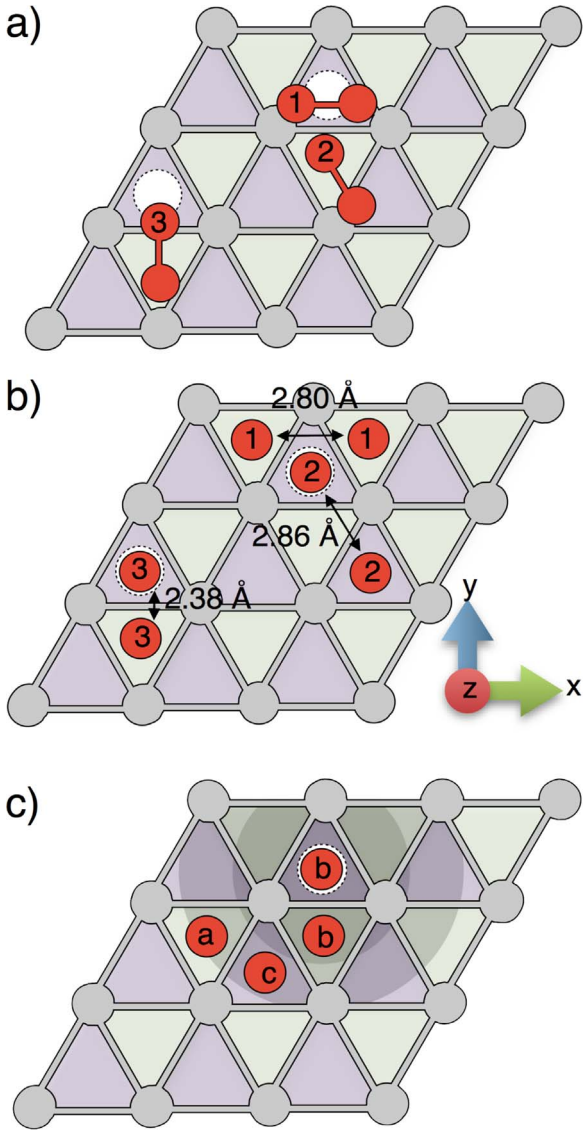

Fig. 7. (a) Schematic top views of the dioxygen molecule deposition on the aluminum surface containing a sub-vacancy schematized by a white circle and (b) final dissociated and adsorbed configurations where identical number belongs to the same molecule. Final adsorption energies are provided in Table 4. (c) Schematic top view of the deposition of atomic oxygen on the aluminum surface containing a sub-vacancy. Letters are oxygen atoms classification in function of ΔH given in Table 5.

Table 6
Energy gain after the adsorption of the dioxygen molecule close to an adatom, in relation with the Fig. 10b.

Positions (#)	1	2	3	4	5	6	7	8
ΔH (eV)	-9.81	-9.15	-9.00	-8.51	-8.47	-6.83	-3.07	-1.83

Table 7
Energy gain after the adsorption of the atomic oxygen close to an ad-atom, in relation with the Fig. 10d.

Positions (#)	a	b	c
ΔH (eV)	-4.38	-4.36	-2.34

sub-surface vacancy as the adsorption energy is the same as the one observed on clean surface. On the contrary, fcc site near the sub-surface vacancy is slightly destabilized by 0.10 eV (b on Fig. 7c). The

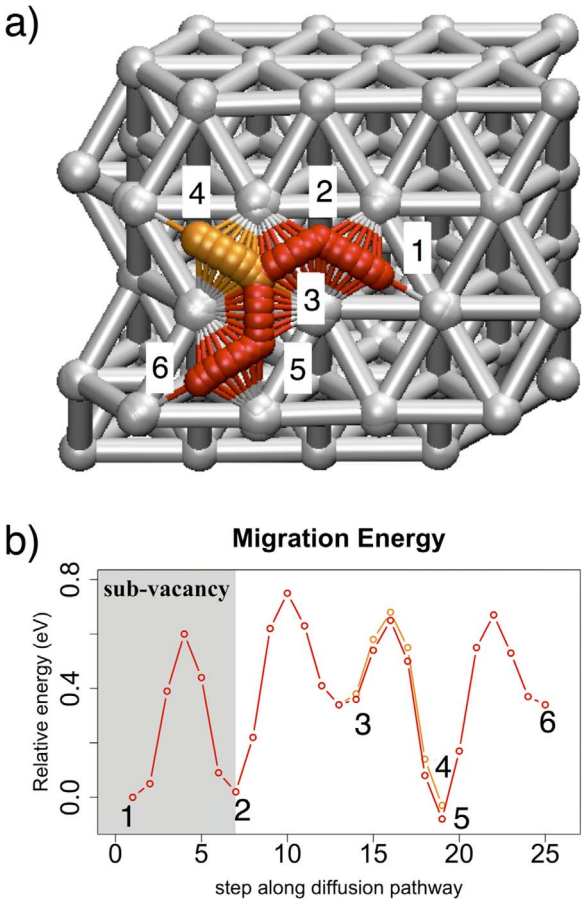

Fig. 8. (a) Top view of the diffusion path of the atomic oxygen close and above the aluminum surface with the sub-surface vacancy located below the position c. (b) Minimum energy path associated to the atomic oxygen migration path in (a). The grey zone corresponds to the surface area above the sub-vacancy defect.

major observation is the drastic change in the oxygen atom stability right above the sub-vacancy on the hcp site. A large energy gain of -0.40 eV is observed compared to clean surface. In this configuration, hcp site features the same stability as the fcc site. This stabilization of the hcp site is also slightly observed for further hcp sites (ΔH=-4.46 eV compared to -4.41 eV).

Migration of the oxygen atom in close vicinity and above the sub-vacancy is plotted on Fig. 8. The starting considered point is the hcp site right above the sub-surface vacancy (position c). As predicted in the stability discussion, this site is as stable as a fcc site, and results in a large increase of the diffusion barrier from 0.30 eV to 0.60 eV compared to clean surface. Others barriers are similar to the surface barriers observed for clean surface, with small shifts because of the electronic perturbation of the sub-vacancy and destabilization of fcc site around this defect.

A deep change in the hcp stability has been observed due to the presence of sub-surface vacancy. Here hcp site becomes isoenergetic with fcc sites, which will drastically slow down oxygen atom migration on the surface. Because of the reduced diffusion of oxygen atom on this surface topology, sub-surface vacancy area can become a center for oxygen island formation.

4.3. Al ad-atom on aluminum surface

We investigate the effect of an aluminum ad-atom on the surface. To do so, we first discuss the existence of such a defect and how an aluminum ad-atom can be formed on the aluminum surface. A Schottky defect requires a high formation energy of 1.79 eV.

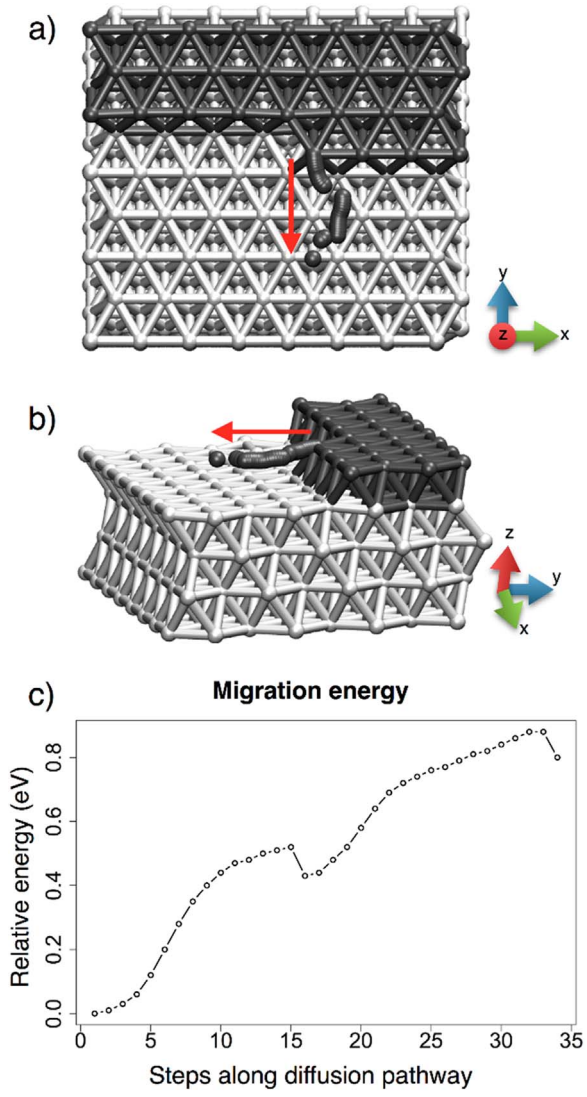

Fig. 9. Formation of an aluminum ad-atom from a surface step at a kink site (a) top view and (b) side view of the step defect with the drag applied in y-axis, on an aluminum located at a kink site (c) energy barrier associated to the drag method.

Furthermore, Aluminum(111) surfaces are also characterized by terraces and kinks [21,40] from where aluminum ad-atom can be generated. In the following we investigate the formation of an ad-atom from a kink site. In this paragraph, a larger slab, four times bigger (64 atoms per layer) than the one previously used was created to avoid limits of calculations due to periodic conditions. A kink defect was simulated by removing half of the aluminum atoms from a (-1-11) vicinal plane as densest atomic planes (Fig. 9a). The Al atom located at the kink site has been constrained to move away from the terrace using a drag method by keeping fixed one coordinate along the migration path (y-axis) while other coordinates are allowed to relax, until the isolation of the aluminum atom from the border of the terrace (Fig. 9). In order to check both the minimum energy path and the saddle point identified by the drag method, the activation barriers have been validated by a NEB calculation.

When looking at Fig. 9, we observe that ad-atom birth occurs through a migration barrier of 0.85 eV, where the dragged aluminum atom goes straight away from the terrace until a stable position is reached as non affected by the terrace proximity. The dragged oxygen atom tends to keep interaction with the terrace when at the fifteenth step, a stabilization of -0.08 eV is observed when oxygen atom relaxes into at the edge of the terrace. At this step, the emerging ad-atom is still affected by the terrace and the drag is pursued along y-axis, until reaching a stable position where the influence of the terrace presence is over. Finally the ad-atom relaxes in a bridge position at 4.70 Å away from the terrace. The final reached position is less stable by 0.80 eV compared to the starting point. A static study was also performed in order to check the stability of states encountered during the extracting process by putting the aluminum atom on different surface sites. The influence of the terrace is felt until a position far from the terrace between 4.52 Å if the aluminum atom is adsorbed on hcp and 4.75 Å if the aluminum atom is adsorbed as a bridge position, in agreement with the identified path. Below these distances, the aluminum atom influenced by the terrace migrates spontaneously to the fcc site on first neighbor site of the terrace associated to an adsorbed energy large of -1.94 eV. Out of this influence, the adsorption energy is -1.24 eV, identical to the clean surface. Once isolated, on a bridge position, this aluminum ad-atom has the ability to diffuse on the surface with a low activation barrier of 0.03 eV. These calculations prove that aluminum ad-atoms can arise from terraces and Schottky defects and justify the following discussion.

A static study on the adsorption of atomic oxygen atom has been conducted to investigate the probability of presence of atomic oxygen atom at the edge of terrace defect. These calculations show that at the bottom of the step, the adsorption energies are -3.99 eV and -4.63 eV on the hcp and fcc sites respectively and at the top and at the edge of the terrace, the adsorption energies are -4.48 eV and -4.77 eV on the hcp and fcc sites respectively. The general observed trend is that the calculated adsorption energies are less favorable than adsorption of oxygen atom on perfect part of the surface without terrace. These results do not show any favorable adsorbed sites for oxygen atoms at the border of a terrace defect indicating a low presence of oxygen species close to such defects.

On an aluminum ad-atom defect, molecular oxygen is adsorbed. Here again, fully dissociated configurations are the most stable (#1 Fig. 10b) where both oxygen atoms are located on close fcc sites with ΔH=-9.81 eV. On this configuration the ad-atom moves far from its initial position to a second neighbor site as explained by the low diffusion energy of the aluminum atom of E_{ac}=0.03 eV and by the lower interaction energy between ad-atom and Al surface compared to oxygen atom with Al surface. The starting configuration leading to this stable state is when molecular oxygen is placed in the far vicinity (second neighbor) of the ad-atom, enabling the molecular oxygen to react with the clean part of the surface. We can notice that in this configuration ΔH is the same as the dissociated molecular dioxygen on clean surface, so there is no interaction between the ad-atom and the oxygen atoms in this configuration as second neighbors. Configurations #7 and #8 are not dissociated states associated to the smaller obtained ΔH where oxygen molecule is adsorbed on top configurations on the ad-atom.

Finally, many of the tested configurations when molecular oxygen is placed in the close neighborhood of the ad-atom lead to non-fully dissociated and bridging configurations where ad-atom is linked to the surface using also aluminum-oxygen-aluminum bonds in addition to Al–Al bonds: Configurations #2, #3, #4, #5 & #6 are also dissociated with at least, one oxygen atom bridged to the ad-atom. We can notice that in many of the observed final configurations, ad-atom is located on bridge configuration (configurations #2, #5, #6). Configuration #6 is less stable because of the oxygen atom remaining as on top metastable position above the ad-atom.

To conclude, we observe that adsorption of oxygen molecule on ad-atom defect is not as favorable energetically as on clean part of Al(111) surface, since oxygen atom will bond with the ad-atom and will form bridged adsorbed state on the surface. To reach those specific bridged states, adsorption on ad-atom must occur on close neighborhood, with an oxygen molecule located above the ad-atom. Furthermore a destabilization of the aluminum ad-atom is observed when oxygen molecule approaches this area (adsorption #1) due to the low interac-

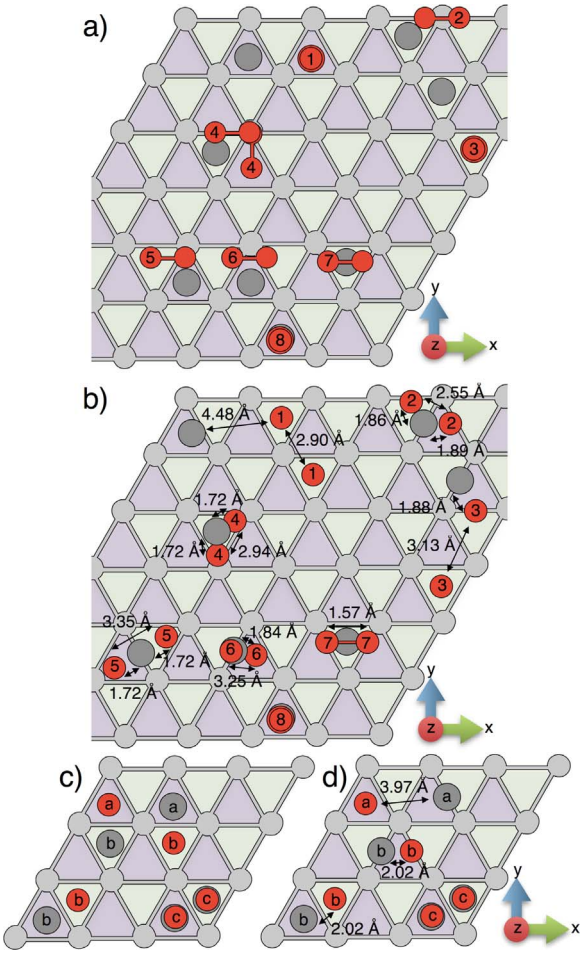

Fig. 10. (a) Schematic top views of dioxygen molecule deposited on the aluminum surface containing an ad-atom schematized by a grey circle and (b) final adsorbed configurations where identical number belongs to the same molecule. Molecules with identical number on starting positions lead to the same final configuration. (c) Schematic top views of atomic oxygen deposition on the aluminum surface and (d) final adsorbed configurations where identical letter belongs to configurations with the same adsorbed energy.

tion of the aluminum ad-atom with the surface compared to the great interaction of oxygen atom with the surface and the already mentioned high velocity of ad-atom on the surface. Here the ad-atom prefers to move away further from the arriving oxygen molecule, to let it react with a clean part of the surface. Furthermore considering the low probability of Al ad-atom to be generated on the surface estimated at 10^{-15} using the transition state theory [63] with an average value of formation energy of 0.85 eV and at room temperature. This probability is also dependent on the surface state of the substrate since it is related to the presence of kink sites. Moreover, if one considers a molecular flux of oxygen species [63], the probability to react with a specific site on the surface is of the order of 10^{-4} when considering room temperature and a given pressure of 0.000133 Pa [40]. Considering these assumptions, the probability of an oxygen molecule to react with ad-atom defect appears to be low in the order of 10^{-20} compared to other possible surface mechanisms.

Ad-atom defects will nevertheless affect the stability of oxygen atom on Al(111) surface: because of the low interaction of aluminum atom on the surface and the high mobility of this ad-atom when isolated on the surface, an oxygen atom diffusing close to the ad-atom will trap this latter to form stable Al–O bonds as a bridged configuration. Indeed, we observe that configuration with one oxygen atom stabilized as bridge with an ad-atom (Fig. 10c and d) has the same stability as adsorbed on hcp (-4.37 eV) as on clean Al(111). Then when moving oxygen atom on the surface, ad-atom diffuse with the oxygen atom keeping the favorable interacting energy. This behavior has already been reported in previous study [62]. We also perform calculations on coupling a vacancy and an Al ad-atom on the surface mimicking a surface Schottky defect. As the main results fit with what has been highly detailed above, we do not enter in details for this specific case. Interestingly, we notice in some adsorptions that dissociation of oxygen molecule destabilizes ad-atom as seen above, and the high mobility of the Al isolated atom will lead to the regeneration of the surface as a barrierless mechanism with the ad-atom healing the vacancy. This process is highly favorable with large enthalpies of around -10 eV, - 11 eV.

5. Conclusion

In this paper we propose a detailed and exhaustive study of oxygen species adsorption and behavior at the surface of perfect and defective Al(111) surfaces. A list of configurations, behaviors and their associated energies is provided with a particular focus given on the variation of kinetics in diffusion of oxygen atom when evolving in close neighborhood of structural defects. This study enables us to have a better understanding on what happens on the Al(111) surface during oxygen deposition or on how oxygen specie reacts with aluminum substrate when taking into account a more realistic surface, i.e. containing defect. Oxygen atom will preferentially migrate on the Al(111) surface using typical fcc to hcp sites through thermal activated mechanism calculated as 0.72 eV and 0.30 eV from fcc to hcp and from hcp to fcc respectively. We observe that once small oxygen islands begin to form on the surface, oxygen atom mobility is reduced because of the interaction energy that will favor oxygen species clustering on the surface. The vacancy and sub-vacancy defects will drastically modify kinetics by slowing down the diffusion of oxygen atom in the vicinity of such defects but their effect is only effective on a local neighborhood of the defects. Hcp sites are stabilized becoming as stable as fcc sites, resulting in possible sites for oxygen island nucleation. On the contrary, terraces do not seem to stabilize oxygen atom, which will prefer to proceed and diffuse on clean part of the aluminum substrate.

Acknowledgment

The authors would like to thank Alain ESTEVE and Mehdi DJAFARI ROUHANI from LAAS-CNRS for discussions. The computer simulations were performed using HPC resources from CALMIP (Grant 1418).

References

[1] S. Schiller, U. Heisig, C. Korndörfer, G. Beister, J. Reschke, K. Steinfelder, J. Strümpfel, Reactive dc high-rate sputtering as production technology, Surf. Coat. Technol. 33 (1987) 405–423. http://dx.doi.org/10.1016/0257-8972(87)90206-4.
[2] W.D. Sproul, New routes in the preparation of mechanically hard films, Science 273 (1996) 889. http://dx.doi.org/10.1126/science.273.5277.889.
[3] A.H. Heuer, D.B. Hovis, J.L. Smialek, B. Gleeson, Alumina scale formation: a new perspective: alumina scale formation: a new perspective, J. Am. Ceram. Soc. 94 (2011) s146–s153. http://dx.doi.org/10.1111/j.1551-2916.2011.04573.x.
[4] B. Lee, G. Mordi, M.J. Kim, Y.J. Chabal, E.M. Vogel, R.M. Wallace, K.J. Cho, L. Colombo, J. Kim, Characteristics of high-k Al2O3 dielectric using ozone-based atomic layer deposition for dual-gated graphene devices, Appl. Phys. Lett. 97 (2010) 043107. http://dx.doi.org/10.1063/1.3467454.
[5] H.X. Li, V.S. Rudnev, X.H. Zheng, T.P. Yarovaya, R.G. Song, Characterization of Al2O3 ceramic coatings on 6063 aluminum alloy prepared in borate electrolytes by micro-arc oxidation, J. Alloy. Compd. 462 (2008) 99–102. http://dx.doi.org/10.1016/j.jallcom.2007.08.046.
[6] O. Benka, M. Steinbatz, Oxidation of aluminum studied by secondary electron emission, Surf. Sci. 525 (2003) 207–214.
[7] V. Zhukov, I. Popova, V. Fomenko, J.T. Yates Jr., Oxygen adsorption on Al(111) – role of surface pretreatment in governing oxidation, Surf. Sci. 441 (1999) 240–250. http://dx.doi.org/10.1016/S0039-6028(99)00613-5.
[8] G. Kresse, J. Hafner, Ab initio molecular dynamics for liquid metals, Phys. Rev. B 47 (1992) 558–561. http://dx.doi.org/10.1103/PhysRevB.47.558.
[9] H.J. Monkhorst, J.D. Pack, Special points for Brillouin-zone integrations, Phys. Rev. B 13 (1976) 5188. http://dx.doi.org/10.1103/PhysRevB.13.5188.

[10] G. Henkelman, G. Jóhannesson, H. Jónsson, Methods for finding saddle points and minimum energy paths, in: Theoretical Methods in Condensed Phase Chemistry, Springer, 2002, pp. 269–302. ⟨http://link.springer.com/chapter/10.1007/0-306-46949-9_10⟩
[11] D. Sheppard, R. Terrell, G. Henkelman, Optimization methods for finding minimum energy paths, J. Chem. Phys. 128 (2008) 134106. http://dx.doi.org/10.1063/1.2841941.
[12] J. Jacobsen, B. Hammer, K.W. Jacobsen, J.K. Norskov, et al., Electronic structure, total energies, and STM images of clean and oxygen-covered Al(111), Phys. Rev. B 52 (1995) 14954. http://dx.doi.org/10.1103/PhysRevB.52.14954.
[13] F. Reichel, L.P.H. Jeurgens, E.J. Mittemeijer, The effect of substrate orientation on the kinetics of ultra-thin oxide-film growth on Al single crystals, Acta Mater. 56 (2008) 2897–2907. http://dx.doi.org/10.1016/j.actamat.2008.02.031.
[14] N. Cai, G. Zhou, K. Müller, D.E. Starr, Tuning the limiting thickness of a thin oxide layer on Al(111) with oxygen gas pressure, Phys. Rev. Lett. 107 (4) (2011) 035502. http://dx.doi.org/10.1103/PhysRevLett.107.035502.
[15] N. Cabrera, N.F. Mott, Theory of the oxidation of metals, Rep. Prog. Phys. 12 (1949) 163. http://dx.doi.org/10.1088/0034-4885/12/1/308.
[16] D. Costa, T. Ribeiro, F. Mercuri, G. Pacchioni, P. Marcus, Atomistic modeling of corrosion resistance: a first principles study of O_2 reduction on the Al(111) surface covered with a thin hydroxylated alumina film, Adv. Mater. Interfaces 1 (2014) 1300072. http://dx.doi.org/10.1002/admi.201300072.
[17] E. Wallin, J.M. Andersson, E.P. Münger, V. Chirita, U. Helmersson, Ab initio studies of Al, O, and O2 adsorption on α – Al2O3 (0001) surfaces, Phys. Rev. B 74 (9) (2006) 125409. http://dx.doi.org/10.1103/PhysRevB.74.125409.
[18] R.C.R. Santos, E. Longhinotti, V.N. Freire, R.B. Reimberg, E.W.S. Caetano, Elucidating the high-k insulator α-Al2O3 direct/indirect energy band gap type through density functional theory computations, Chem. Phys. Lett. 637 (2015) 172–176. http://dx.doi.org/10.1016/j.cplett.2015.08.004.
[19] M. Koberidze, A.V. Feshchenko, M.J. Puska, R.M. Nieminen, J.P. Pekola, Effect of interface geometry on electron tunnelling in Al/Al_2O_3/Al junctions, J. Phys. Appl. Phys. 49 (2016) 165303. http://dx.doi.org/10.1088/0022-3727/49/16/165303.
[20] G. Pilania, B.J. Thijsse, R.G. Hoagland, I. Lazić, S.M. Valone, X.-Y. Liu, Revisiting the Al/Al2O3 interface: coherent interfaces and misfit accommodation, Sci. Rep. 4 (2014) 9. http://dx.doi.org/10.1038/srep04485.
[21] H. Brune, J. Wintterlin, J. Trost, G. Ertl, J. Wiechers, R.J. Behm, Interaction of oxygen with Al(111) studied by scanning tunneling microscopy, J. Chem. Phys. 99 (1993) 2128–2148. http://dx.doi.org/10.1063/1.465278.
[22] C. Lanthony, J.M. Ducéré, M.D. Rouhani, A. Hemeryck, A. Estève, C. Rossi, On the early stage of aluminum oxidation: an extraction mechanism via oxygen cooperation, J. Chem. Phys. 137 (2012) 094707. http://dx.doi.org/10.1063/1.4746943.
[23] C. Lanthony, J.-M. Ducéré, A. Estève, C. Rossi, M. Djafari-Rouhani, Formation of Al/CuO bilayer films: basic mechanisms through density functional theory calculations, Thin Solid Films 520 (2012) 4768–4771. http://dx.doi.org/10.1016/j.tsf.2011.10.184.
[24] J.X. Guo, L.J. Wei, D.Y. Ge, L. Guan, Y.L. Wang, B.T. Liu, Dissociation and reconstruction of O2 on Al(111) studied by first-principles, Appl. Surf. Sci. 264 (2013) 247–254. http://dx.doi.org/10.1016/j.apsusc.2012.10.010.
[25] T. Kuschel, A. von Keudell, Ion-enhanced oxidation of aluminum as a fundamental surface process during target poisoning in reactive magnetron sputtering, J. Appl. Phys. 107 (2010) 103302. http://dx.doi.org/10.1063/1.3415531.
[26] I. Popova, V. Zhukov, J.T. Yates, Comparative study of Al(111) oxidation with O3 and O2, Surf. Sci. 518 (2002) 39–48. http://dx.doi.org/10.1016/S0039-6028(02)02064-2.
[27] A. Arranz, C. Palacio, Characterization of the surface and interface species formed during the oxidation of aluminum, Surf. Sci. 355 (1996) 203–213. http://dx.doi.org/10.1016/0039-6028(96)01056-4.
[28] A. Hasnaoui, O. Politano, J.M. Salazar, G. Aral, Nanoscale oxide growth on Al single crystals at low temperatures: variable charge molecular dynamics simulations, Phys. Rev. B 73 (13) (2006) 035427. http://dx.doi.org/10.1103/PhysRevB.73.035427.
[29] L.C. Ciacchi, M.C. Payne, Hot-atom O2 dissociation and oxide nucleation on Al(111), Phys. Rev. Lett. 92 (2004). http://dx.doi.org/10.1103/PhysRevLett.92.176104.
[30] Y.F. Zhukovskii, P.W.M. Jacobs, M. Causá, On the mechanism of the interaction between oxygen and close-packed single-crystal aluminum surfaces, J. Phys. Chem. Solids 64 (2003) 1317–1331. http://dx.doi.org/10.1016/S0022-3697(03)00156-2.
[31] K. Honkala, K. Laasonen, Oxygen molecule dissociation on the Al(111) surface, Phys. Rev. Lett. 84 (2000) 705. http://dx.doi.org/10.1103/PhysRevLett.84.705.
[32] A.J. Komrowski, J.Z. Sexton, A.C. Kummel, M. Binetti, O. Weiße, E. Hasselbrink, Oxygen Abstraction from dioxygen on the Al(111) surface, Phys. Rev. Lett. 87 (2001). http://dx.doi.org/10.1103/PhysRevLett.87.246103.
[33] D.E. Oner, B. Kasemo, I. Zorić, On the role of long-range elastic interactions for the Al(111) oxide nucleation kinetics, Surf. Sci. 545 (2003) L761–L766. http://dx.doi.org/10.1016/j.susc.2003.07.015.
[34] T. Sasaki, T. Ohno, Dissociation process of O2 on the Al(111) surface, Surf. Sci. 433 (1999) 172–175. http://dx.doi.org/10.1016/S0039-6028(99)00056-4.
[35] M. Schmid, G. Leonardelli, R. Tscheliessnig, A. Biedermann, P. Varga, Oxygen adsorption on Al(111): low transient mobility, Surf. Sci. 478 (2001) L355–L362. http://dx.doi.org/10.1016/S0039-6028(01)00967-0.
[36] A. Kiejna, B.I. Lundqvist, Stability of oxygen adsorption sites and ultrathin aluminum oxide films on Al(111), Surf. Sci. 504 (2002) 1–10. http://dx.doi.org/10.1016/S0039-6028(02)01155-X.
[37] T. Sasaki, T. Ohno, Adsorption of the oxygen to the Al(111) surface, Comput. Mater. Sci. 14 (1999) 8–12. http://dx.doi.org/10.1016/S0927-0256(98)00065-2.
[38] F. Libisch, C. Huang, P. Liao, M. Pavone, E.A. Carter, Origin of the energy barrier to chemical reactions of O2 on Al(111): evidence for charge transfer, not spin selection, Phys. Rev. Lett. 109 (5) (2012) 198303. http://dx.doi.org/10.1103/PhysRevLett.109.198303.
[39] L. Österlund, I. Zoric-Acute, B. Kasemo, Dissociative sticking of O2 on Al(111), Phys. Rev. B 55 (1997) 15452. http://dx.doi.org/10.1103/PhysRevB.55.15452.
[40] J. Trost, H. Brune, J. Wintterlin, R.J. Behm, G. Ertl, Interaction of oxygen with Al(111) at elevated temperatures, J. Chem. Phys. 108 (1998) 1740–1747. http://dx.doi.org/10.1063/1.475546.
[41] R. Chakarova, D.E. Oner, I. Zorić, B. Kasemo, Monte Carlo simulation of initial Al(111) oxidation, Surf. Sci. 472 (2001) 63–79. http://dx.doi.org/10.1016/S0039-6028(00)00923-7.
[42] D.E. Oner, H. Ternow, R. Chakarova, B. Kasemo, I. Zorić, Al(111) oxidation kinetics in the submonolayer regime; experiment and Monte Carlo simulations, Surf. Sci. 512 (2002) L325–L330. http://dx.doi.org/10.1016/S0039-6028(02)01683-7.
[43] Y. Yourdshahyan, B. Razaznejad, B.I. Lundqvist, Adiabatic potential-energy surfaces for oxygen on Al(111), Phys. Rev. B 65 (17) (2002) 075416. http://dx.doi.org/10.1103/PhysRevB.65.075416.
[44] C. Lanthony, M. Guiltat, J.M. Ducéré, A. Verdier, A. Hémeryck, M. Djafari-Rouhani, C. Rossi, Y.J. Chabal, A. Estève, Elementary surface chemistry during CuO/Al nanolaminate-thermite synthesis: copper and oxygen deposition on aluminum(111) surfaces, ACS Appl. Mater. Interfaces (2014). http://dx.doi.org/10.1021/am503126k.
[45] D.E. Oner, R. Chakarova, I. Zorić, B. Kasemo, Monte Carlo simulation of the chemisorption kinetics and initial oxide formation on Al(111), J. Chem. Phys. 113 (2000) 8869. http://dx.doi.org/10.1063/1.1326028.
[46] H.M. Polatoglou, M. Methfessel, M. Scheffler, Vacancy-formation energies at the (111) surface and in bulk Al, Cu, Ag, and Rh, Phys. Rev. B 48 (1993) 1877. http://dx.doi.org/10.1103/PhysRevB.48.1877.
[47] V.P. Zhdanov, B. Kasemo, Simulation of the first stage of oxide formation on Al(111), Surf. Sci. 521 (2002) L662–L668. http://dx.doi.org/10.1016/S0039-6028(02)02331-2.
[48] B.G. Frederick, M.B. Lee, N.V. Richardson, A vibrational characterisation of the O/Al(111) system: a reassignment of HREELS data, Surf. Sci. 348 (1996) 71–74. http://dx.doi.org/10.1016/0039-6028(95)01101-3.
[49] L.P.H. Jeurgens, W.G. Sloof, F.D. Tichelaar, E.J. Mittemeijer, Growth kinetics and mechanisms of aluminum-oxide films formed by thermal oxidation of aluminum, J. Appl. Phys. 92 (2002) 1649. http://dx.doi.org/10.1063/1.1491591.
[50] C. Carbogno, J. Behler, K. Reuter, A. Groß, Signatures of nonadiabatic O 2 dissociation at Al(111): first-principles fewest-switches study, Phys. Rev. B 81 (12) (2010) 035410. http://dx.doi.org/10.1103/PhysRevB.81.035410.
[51] M.L. Neuburger, D.P. Pullman, On the viability of single atom abstraction in the dissociative chemisorption of O2 on the Al(111) surface, J. Chem. Phys. 113 (2000) 1249. http://dx.doi.org/10.1063/1.481902.
[52] C. Lanthony, M. Guiltat, J.M. Ducéré, A. Verdier, A. Hémeryck, M. Djafari-Rouhani, C. Rossi, Y.J. Chabal, A. Estève, Elementary surface chemistry during CuO/Al nanolaminate-thermite synthesis: copper and oxygen deposition on aluminum (111) surfaces, ACS Appl. Mater. Interfaces 6 (2014) 15086–15097. http://dx.doi.org/10.1021/am503126k.
[53] A. Kiejna, B.I. Lundqvist, First-principles study of surface and subsurface O structures at Al(111), Phys. Rev. B 63 (10) (2001) 085405. http://dx.doi.org/10.1103/PhysRevB.63.085405.
[54] J.P. Perdew, K. Burke, M. Ernzerhof, Generalized gradient approximation made simple, Phys. Rev. Lett. 77 (1996) 3865. http://dx.doi.org/10.1103/PhysRevLett.77.3865.
[55] G. Kresse, J. Furthmüller, Efficiency of ab-initio total energy calculations for metals and semiconductors using a plane-wave basis set, Comput. Mater. Sci. 6 (1996) 15–50. http://dx.doi.org/10.1016/0927-0256(96)00008-0.
[56] G. Kresse, J. Furthmüller, Efficient iterative schemes for ab initio total-energy calculations using a plane-wave basis set, Phys. Rev. B 54 (1996) 11169. http://dx.doi.org/10.1103/PhysRevB.54.11169.
[57] G. Kresse, J. Hafner, Ab initio molecular-dynamics simulation of the liquid-metal–amorphous-semiconductor transition in germanium, Phys. Rev. B 49 (1994) 14251. http://dx.doi.org/10.1103/PhysRevB.49.14251.
[58] G. Henkelman, B.P. Uberuaga, H. Jónsson, A climbing image nudged elastic band method for finding saddle points and minimum energy paths, J. Chem. Phys. 113 (2000) 9901. http://dx.doi.org/10.1063/1.1329672.
[59] G. Katz, R. Kosloff, Y. Zeiri, Abstractive dissociation of oxygen over Al(111): a nonadiabatic quantum model, J. Chem. Phys. 120 (2004) 3931. http://dx.doi.org/10.1063/1.1635360.
[60] H. Brune, J. Wintterlin, R.J. Behm, G. Ertl, Surface migration of "'hot'" adatoms in the course of dissociative chemisorption of oxygen on Al(111), Phys. Rev. Lett. 68 (1992) 624–626. http://dx.doi.org/10.1103/PhysRevLett.68.624.
[61] M. Kerkar, D. Fisher, D.P. Woodruff, B. Cowie, Adsorption site determination for oxygen on AI(111) using normal incidence standing X-ray wavefield absorption, Surf. Sci. 271 (1992) 45–56. http://dx.doi.org/10.1016/0039-6028(92)90860-9.
[62] A. Migaou, B. Sarpi, M. Guiltat, K. Payen, R. Daineche, G. Landa, S. Vizzini, A. Hémeryck, A perfect wetting of Mg monolayer on Ag(111) under atomic scale investigation: first principles calculations, scanning tunneling microscopy, and Auger spectroscopy, J. Chem. Phys. 144 (2016) 194708. http://dx.doi.org/10.1063/1.4949764.
[63] A. Hémeryck, A. Estève, N. Richard, M. Djafari Rouhani, G. Landa, A kinetic Monte Carlo study of the initial stage of silicon oxidation: basic mechanisms-induced partial ordering of the oxide interfacial layer, Surf. Sci. 603 (2009) 2132. http://dx.doi.org/10.1016/j.susc.2009.04.014.